Heterotrophic prokaryote distribution along a 2,300 km transect in the North Pacific subtropical gyre during strong La Niña conditions: relationship between distribution and hydrological conditions

M. GIRAULT[1], H. ARAKAWA[2], A. BARANI[3], H. J. CECCALDI[3], F. HASHIHAMA[2], and G. GREGORI[3]

[1]{Kanagawa Academy of Science and Technology, LISE 4C-3, 3-25-13 Tonomachi Kawasaki-ku, Kawasaki-shi, Kanagawa 210-0821, Japan.}

[2]{Department of Ocean Sciences, Tokyo University of Marine Science and Technology, 5-7 Konan 4, Minato-ku, Tokyo 108-8477, Japan.}

[3]{Aix-Marseille Université, Mediterranean Institute of Oceanography MIO UM 110, Université de Toulon, CNRS/INSU, IRD, 13288, Marseille, cedex 09, France.}

Correspondence to: M. GIRAULT (girault.bmi@gmail.com; gerald.gregori@univ-amu.fr)

Abstract

The spatial distribution of heterotrophic prokaryotes was investigated during the Tokyo–Palau cruise in the western part of the North Pacific subtropical gyre (NPSG) along a north–south transect between 33.60 and 13.25° N. The cruise was conducted in three different hydrological areas identified as the Kuroshio region, the Subtropical gyre area and the Transition zone. Two eddies were crossed along the transect: one cold core cyclonic eddy and one warm core anticyclonic eddy and distributions of the heterotrophic prokaryotes were recorded. By using analytical flow cytometry and a nucleic acid staining protocol, heterotrophic prokaryotes were discriminated into three subgroups depending on their nucleic acid content (low, high and very high nucleic acid contents labeled LNA, HNA

and VHNA, respectively). Statistical analyses performed on the dataset showed that LNA, mainly associated with low temperature and low salinity, were dominant in all the hydrological regions. In contrast, HNA distribution seemed to be associated with temperature, salinity, Chl *a* and silicic acid. A latitudinal increase in the HNA/LNA ratio was observed along the north–south transect and was related to higher phosphate and nitrate concentrations. However, the opposite relationship observed for the VHNA/HNA ratio suggested that the link between nucleic acid content and oligotrophic conditions is not linear, underlying the complexity of the biodiversity in the VHNA, HNA and LNA subgroups. In the Kuroshio Current, it is suggested that the high concentration of heterotrophic prokaryotes observed at station 4 was linked to the path of the cold cyclonic eddy core. In contrast, it is thought that low concentrations of heterotrophic prokaryotes in the warm core of the anticyclonic gyre (Sta. 9) are related to the low nutrient concentrations measured in the seawater column. Our results showed that the high variability between the various heterotrophic prokaryote cluster abundances depend both on the mesoscale structures and the oligotrophic gradient.

1 Introduction

Marine heterotrophic prokaryotes play a key role in pelagic ecosystems both in terms of carbon sequestration and organic matter remineralisation. Their distribution is controlled by biotic (bottom-up control, top-down control by grazing, virus lyses) and abiotic variables (temperature, salinity, pressure, irradiance, nutrient concentrations). These possible limiting variables are shared with the autotrophic community and competition for resources inevitably occurs in order for each to survive in the same pelagic ecosystem. Competition between heterotrophic prokaryotes and phytoplankton for different forms of inorganic nitrogen and phosphorus has been clearly demonstrated both in laboratory experiments and in the open ocean (Currie and Kalff, 1984; Vadstein, 1998; Thingstad et al., 1998). Moreover, several studies have reported that dissolved organic compounds can be an alternative nutrient source for some nutrient-stressed phytoplankton (Duhamel et al., 2010; Girault et al., 2013a). The common utilization of the inorganic and/or organic matter, such as dissolved organic phosphorus, could lead to a tight coupling between the heterotrophic prokaryotes and photoautotrophs along an oligotrophic gradient. However, the relationship between heterotrophic prokaryote abundance and oligotrophic conditions is unclear, especially in terms of mesoscale structures such as eddies (Baltar et al., 2010; Lasternas et

al., 2013). The differences within the same type of mesoscale circulation reported in the literature highlights that the relationship between heterotrophic prokaryotes and photoautotrophs can be dependent on the identification of the different microorganisms making up the community (Girault et al., 2013b).

In this study, using analytical flow cytometry combined with fluorescent dyes we were able to identify three different subgroups among the bulk of heterotrophic prokaryotes: a group characterized by a very high nucleic acid content (VHNA), another by a high nucleic acid content (HNA), and finally a group with a low nucleic acid content (LNA). Previous studies have reported that the more active microorganisms seem to have the higher nucleic acid contents (Gasol et al., 1999; Lebaron et al., 2001). Complementary results have suggested that heterotrophic prokaryote activities are influenced by environmental parameters especially under oligotrophic conditions (Zubkov et al., 2001; Grégori et al., 2001, 2003a; Nishimura et al., 2005; Sherr et al., 2006; Bouvier et al., 2007). Using the basis of these previous reports, the oligotrophic conditions investigated in the western part of the NPSG during the Tokyo–Palau Cruise enabled us to examine the relationship between different groups of heterotrophic prokaryotes, as defined by different nucleic acid contents, and their environmental conditions.

Investigations into the heterotrophic prokaryote distribution in the western part of the NPSG are scarce and mostly restricted to the Kuroshio Current or the area near the Japan shelf during El-Niño events (Mitbavkar et al., 2009; Kataoka et al., 2009; Kobari et al., 2011). In contrast, the Tokyo Palau cruise was conducted during a strong LaNiña condition and over a large latitudinal gradient to include various seawater masses. In this work, we studied the extent to which abundance and distribution of various heterotrophic prokaryotic groups, defined by flow cytometry (VHNA, HNA, LNA) were influenced by phytoplankton distribution and environmental variables. The relationships between each heterotrophic prokaryote group and two different mesoscale eddies (one anticyclonic and one cyclonic) were also examined in order to identify any modification in organism distribution which could be related to the oligotrophic conditions found during the cruise.

2 Materials and methods

2.1 Study area and sample collection

This study was conducted from 17 January to 8 February 2011 on board RT/V Shinyo Maru during the Tokyo–Palau cruise. Samples were collected in the western part of the NPSG between 33.60 and 13.25° N along the 141.5° E transect (Fig. 1). Twelve stations (Sta.) were sampled using 2.5 L Niskin bottles mounted on a rosette frame equipped with the Conductivity–Temperature–Depth (CTD) and in situ fluorometer system. Seawater was sampled without replicates at several depths between the surface and 200 m. Due to bad weather conditions, the seawater samples between station 1 and 4 were collected only at the surface (3 m) using a single Niskin Bottle. At these 4 stations, eXpendable Conductivity/Temperature/Depth profiling systems (XCTD) were used to measure temperature and salinity. The Brunt-Väisäla buoyancy frequency (N^2) was calculated using the exact thermodynamic expression reported by King et al. (2012) (equation 1).

$$N^2 = g^2\left(\frac{d\rho}{dp} - \frac{1}{c_s^2}\right) \qquad (1)$$

Where $\frac{d\rho}{dp}$ is the vertical gradient of *in-situ* density (ρ). The acceleration (g) due to the gravity was assumed to be constant during the Tokyo-Palau cruise (g=9.81) and the speed of sound (c_s) was calculated depending on the depth, salinity and temperature according to Del Grosso, (1974). The mixed layer depths were estimated as the depths at which the maximum stratification occurred (i.e., maximum of N^2 at each station). The irradiance was monitored at five stations (5, 7, 9, 11, 12) using a Profiling Reflectance radiometer (PRR 600 Biospherical Instrument®). The depth of the euphotic layer was estimated as the depth of 1 % of photosynthetically active radiation at noon.

2.2 Altimetry and large scale climatic conditions

The altimetry data (sea level anomaly) was produced by Ssalto/Duacs and distributed by Aviso, with support from CNES (http://www.aviso.oceanobs.com/duacs/). The sea level anomaly map centered on the 18 January 2011 was plotted using the Panoply software from NASA (http://www.giss.nasa.gov/tools/panoply/). This map was processed by compiling the data collected over a six weeks period before and after the chosen date (Fig. 1). The current sea maps provided by the bulletin of the Japanese coast guard were used to validate the satellite data and display the paths of both the cyclonic gyre and the Kuroshio Stream (http://www1.kaiho.mlit.go.jp/KANKYO/KAIYO/qboc/index_E.html).

2.3 Nutrient analyses

Nutrient samples were collected from Niskin bottles, immediately put into cleaned plastic tubes in the dark, plunged into liquid nitrogen and stored in the deep freeze (−60 ◦C) until analyses. The highly sensitive colorimetric method incorporating the AutoAnalyzer II (SEAL Analytical) and Liquid Waveguide Capillarity Cells (World precision Instruments), was used to determine nutrient concentrations (nitrate + nitrite, soluble reactive phosphorus and silicic acid) according to the methods listed in Hashihama et al. (2009) and Hashihama and Kanda (2010). Seawater collected at the surface of the western part of NPSG, which had been preserved for > 1 year, was used as nitrate + nitrite blank water. The blank water was analyzed using the chemiluminescent method described in Garside (1982). The detection limits for nitrate + nitrite, soluble reactive phosphorus and silicic acid were 3, 3 and 11 nM, respectively. Because soluble reactive phosphorus consists mainly of orthophosphate and nitrite was not substantially detectable, soluble reactive phosphorus and nitrate + nitrite are hereafter referred to as phosphate and nitrate.

The nutrient fluxes into the surface mixed layer were calculated using the equation $K\frac{dNut}{dz}$ where K is the local vertical diffusivity, *Nut* the concentration in nutrients (phosphates, nitrates or silicic acid) and $\frac{dNut}{dz}$ the vertical nutrient gradient. To compensate for irregular sampling depths among the stations, the nutrient profiles were linearly interpolated onto the 1 m grid. Then, vertical nutrient gradients were calculated between sequential depth bins (Painter et al., 2013). This method has the advantage to show the nutrient flux from a particular part of the water column. Due to the lack of an Acoustic Doppler Current Profiler (ADCP) on the ship, the local vertical diffusivity (K) was estimated using the literature (Table 1). Among the K values reported in the oligotrophic conditions, a vertical diffusion coefficient of 0.5 $cm^2.s^{-1}$ was chosen as a standard value (Table 1).

2.4 Chlorophyll *a* and flow cytometry analyses

The depth of the deep chlorophyll a maximum was determined from fluorescence profiles using the pre-calibrated in situ fluorometer. To measure chlorophyll a concentration, 250 cm^3 of seawater was filtrated through Whatman® nucleopore filters (porosity ~ 0.2 µm) using a low vacuum pressure (< 100 mm of Hg). Filters were then immersed into tubes containing N,N-dimethylformamide (DMF)- and stored in the dark at 4° C until analyses on shore.

Chlorophyll a was analysed using a Turner Designs fluorometer pre-calibrated with pure Chl a pigment (Suzuki and Ishimaru, 1990).

Samples for heterotrophic prokaryotes were collected from the Niskin bottles and pre-filtered onto disposable 100 µm porosity nylon filters to prevent clogging of any in the flow cytometer. Seawater aliquots of 1.8 cm3 were fixed with 2 % (w/v final dilution) formaldehyde solution, quickly frozen in liquid nitrogen and stored in the deep freeze onboard (−60 °C) until analysis at the flow cytometry core facility PRECYM of the Mediterranean Institute of Oceanology (http://precym.mio.osupytheas.fr). In the PRECYM, samples were thawed at room temperature and stained using SYBR Green II (Molecular Probes®) methods detailed in Marie et al. (1999), Lebaron et al. (1998) and modified by Grégori et al. (2003b). The analyses were performed on a FACSCalibur flow cytometer (BD Biosciences®) equipped with an air-cooled argon laser (488 nm, 15 mW). For each particle (cell), five optical parameters were recorded: two light scatter signals, namely forward and right angle light scatters and three fluorescences corresponding to emissions in green (515–545 nm), orange (564–606 nm) and red (653–669 nm) wavelength ranges. Data were collected using the CellQuest software (BD Biosciences®) and the analysis and optical resolution of the various groups of heterotrophic prokaryotes were performed a posteriori using the SUMMIT v4.3 software (Beckman Coulter). For each sample, the runtime of the flow cytometer was 2 min and the flow rate set to 50 µL.min−1 (corresponding to the “Med” flow rate of the flow cytometer). Trucount™ calibration beads (Becton Dickinson Biosciences) were also added to the samples just prior to analysis as an internal standard to monitor the instrument stability and accurately determine the volume analyzed. Following the staining of the nucleic acid with SYBR Green II, heterotrophic prokaryotes, excited at 488 nm, were recorded and enumerated according to their right-angle light scatter intensity (SSC) which relates to the cell size and their green fluorescence intensity (515–545 nm) which relates to the nucleic acid content. As already widely described in the literature, several heterotrophic prokaryote groups can be optically resolved by flow cytometry depending on their average green fluorescence intensities related to their nucleic acid content : in this study, a group of cells with a lower green fluorescence corresponding to heterotrophic prokaryotes with a lower nucleic acid content (LNA), a group of cells displaying a higher green fluorescence corresponding to a higher nucleic acid content (HNA) and a last group of cells with the highest green fluorescence intensity corresponding to the highest nucleic acid content (VHNA) (Fig. 2). The overlap between the stained phytoplankton, in particular *Prochlorococcus* and *Synechococcus*, and the heterotrophic prokaryotes (in terms of green fluorescence and side scatter intensity)

was resolved by using red fluorescence (induced by the chlorophyll) to discriminate and identify the photoautotrophs (Sieracki et al., 1995). The heterotrophic prokaryote abundances were also expressed for each cluster (LNA, HNA and VHNA) in terms of carbon biomass using a conversion factor of 15 fg.C.cell^{-1} (Caron *et al.*, 1995).

Although this study focuses on the distribution of the heterotrophic prokaryotes, ultraphytoplankton was also investigated during the Tokyo-Palau project. Briefly, the ultraphytoplankton was sampled thanks to Niskin bottles and filtrated through a 100 µm mesh size. 4.5 cm^{-3} of subsamples preserved with 0.5 cm^{-3} of a 20 % formaldehyde solution (i.e., 2% final concentration) were put into 5 cm^{-3} Cryovials tubes. Similarly to the heterotrophic prokaryote samples, Cryovials tubes were rapidly frozen in liquid nitrogen and stored in a deep freezer (-60 °C) until analysis. Analyses were all performed in the same period than the heterotrophic prokaryotes and based on their light scatter and fluorescence emission properties. Ultraphytoplankton was discriminated in this study into five flow cytometry clusters (*Synechococcus*, *Prochlorococcus*, Picoeukaryotes, Nanoeukaryotes and Nanocyanobacteria-like) as described in Girault et al. (2013b).

2.5 Statistical analysis

To analyse the multivariate data set, principal component analyses (PCA) and redundancy analysis (RDA) were performed using the R software (vegan package) and the Biplot macro for Excel® (Lipkovich and Smith, 2002). PCA was performed in order to qualitatively identify the relationships between heterotrophic prokaryotes and the environmental variables (Pearson, 1901). Possible links between each heterotrophic prokaryote subgroup and their environmental variables were quantitatively examined using the RDA. For the RDA, the data set was log10 (x+1)-transformed to correct for the large differences in scale among the original variables. A Monte-Carlo test was used in order to test the significance of the RDA results. Partial RDAs were also carried out to evaluate the effects of each explanatory variable set on the heterotrophic prokaryote composition (Liu, 1997). The first RDA was performed on the whole data set by taking into account the heterotrophic prokaryotes as one single group. Additional partial RDAs were performed for each subgroup (LNA, HNA, and VHNA). The environmental variables in the additional partial RDAs were classified into three intercorrelated variable groups, namely: the depth-related parameters (phosphate, nitrate, depth), spatial-related parameters (temperature and salinity) and the phytoplankton-related parameters (Chl *a* and silicic acid). This decision was made considering the results of the PCA (environmental variables were separated into three

groups).

3 Results

3.1 Sampling sites and ultraphytoplankton distribution.

The cruise took place along a north–south transect in the western part of the NPSG (141.5° E) during a strong La-Niña climatic event. According to the temperature–salinity diagram presented in the study made by Girault et al. (2013b), three main areas corresponding to the Kuroshio region (Sta. 1–4), the subtropical gyre (Sta. 5–8) and the Transition zone (Sta. 9–12) were discriminated (Fig. 1). The discrimination between the Kuroshio area and the Subtropical gyre seawater masses was confirmed by comparing the Tokyo-Palau data set and the studies of Sekine and Miyamoto (2002) and Kitajima et al. (2009). The cruise crossed two main eddies identified in this study as a cold core cyclonic eddy (C), and a warm core anticyclonic eddy (A) (Fig. 1). Eddy C (31° N, 141° E) is located in the Kuroshio region and eddy A (20.5° N, 142° E) in the Transition zone. The distribution of the ultraphytoplankton assemblages observed during the Tokyo-Palau cruise was reported in detail in the study of Girault et al., (2013b). Briefly, ultraphytoplankton was characterized by an heterogeneous distribution of its phytoplankton groups associated with the complex distribution of the various seawater masses met during the cruise (including salinity front, subtropical countercurrent, eddies). Among the phytoplankton communities *Prochlorococcus* numerically dominated the ultraphytoplankton assemblages in the samples collected in the stratified oligotrophic areas such as the Subtropical gyre area and the Transition zone. Picoeukaryotes, Nanoeukaryotes and *Synechococcus* also constituted a significant part of the carbon biomass in the region depleted in phosphate and nitrate. The role of the cold core eddy C was reported at the surface where the highest concentration of Nanoeukaryotes in the surface sample was found in the very core of the cyclonic eddy (Sta. 3) and where, the *Synechococcus* outnumbered the *Prochlorococcus* abundance in the path of the cold core cyclonic eddy (Sta. 4). The Nanocynaobacteria-like group was reported to be controlled by the frontal system observed at station 9 rather than the concentration of inorganic nutrients.

3.2 Stratification of seawater masses and vertical nutrient fluxes

The Brunt-Väisäla buoyancy frequencies calculated from the CTD data set are characterized

by low N^2 values (<$2x10^{-4}$ s^{-2}) from the surface down to the 90 m depth (Fig. 3). Below this depth, the vertical distribution of N^2 was more irregular and reached at the maximum $1.09x10^{-3}$ s^{-2} at station 11 (90 m). Fig. 3 also shows that the depth of the N^2 maximum (thermocline depth) tended to be shallower in the southernmost part of the transect (Sta. 1, 185 m to Sta. 11, 90 m) underlying the strengthening of the upper thermocline when the heat flux at the surface is positive and wind mixing is low in the South part of the transect. Along the latitudinal transect, two particular values of the thermocline depths were found at station 3 (145 m) and at station 9 (140 m) corresponding to the cyclonic and anticyclonic eddies, respectively. Moreover, excepted at station 3 and station 9, the first increases of N^2 (> $2x10^{-4}$ s^{-2}) from the surface to the 200 m depth corresponded to the depth of the thermocline and indicated the lack of seasonal thermocline as already described in Sprintall and Roemmich (1999). The limit of the euphotic layer (defined by the depth with 1 % of the irradiance at the surface) was also plotted in Fig. 3. During the cruise, this limit varied from 84 m (Sta. 7) to 115 m (Sta. 12). Except station 11, the limit of the euphotic layer was located upper the thermocline. The average of the absolute difference between the euphotic layer and the thermocline depths was 34 ±11 m.

Figure 4 shows the vertical gradient of nutrients (phosphates, nitrates and silicic acid). The vertical phosphate profiles were characterized by a very low gradient (<1 $nM.m^{-1}$) in the upper 100 m from station 6 to station 12. Both positive and negative gradients were observed and no specific distribution between them was found. Under the depth of 100 m, higher phosphate gradients (> 3 $nM.m^{-1}$) were found and defined the phosphacline depths as displayed in Figure 6 of the study made by Girault et al. (2013b). Nitrates showed that vertical profiles closely corresponded to phosphates with negative or positive values lower than 5 $nM.m^{-1}$ and higher gradient below 100 m. The vertical distribution of the silicic acid gradient was more complex with moderate gradients ranging from 0.01 to 0.02 $\mu M.m^{-1}$ were observed in the upper 100 m depth at stations 5, 6, 7, and 12. Similarly to phosphates and nitrates, the highest gradients of silicic acide (0.04 $\mu M.m^{-1}$) were found below 100 m depth from station 6 to station 10. Taking into account all the panels of Figure 4, Station 8 showed a particular pattern between 100 m and 160 m depths where two superimposed high gradients were observed. The depths of these high gradients were found to be similar for phosphates and silicic acid (100-115 m and 130-155 m) but the vertical profile of nitrates gradient showed a slightly lower depth (130-140 m and 155-170 m).

By using a vertical diffusion coefficient of 0.5 $cm^2.s^{-1}$, the nutrient fluxes were calculated

from station 5 to station 11 (Table 2). Phosphate fluxes into the surface mixed layer were negative at stations 5 and 6 (-0.52 and -1.34 µmol.m^{-2}.d^{-1}, respectively) and positive from station 7 to station 11. The positive phosphate fluxes were maximum at station 7 (9.43 µmol.m^{-2}.d^{-1}) and decreased to reach 1.38 µmol.m^{-2}.d^{-1} at station 11. The percentages of diffuse flux per day relative to the standing stock in the mixed layer were particularly low and varied from -0.03 % (Sta. 6) to 0.76 % (Sta. 8). Nitrate fluxes into the mixed layer were positive and highly variable along the transect (~0 to 81.3 µmol.m^{-2}.d^{-1}). The percentage of daily diffuse supply relative to the pool reflects this result and varied from ~0 (Sta. 7 and 10) to 432 % (Sta. 8). The Silicic acid fluxes were globally higher than the phosphate and nitrate fluxes calculated in the mixed layer (up to 571.1 µmol.m^{-2}.d^{-1}; Sta. 9). The daily diffuse supply relative to the mixed layer pool was low and spread from 0.002 % (Sta. 5) to 0.48 % (Sta. 9).

3.3 Distribution of the heterotrophic prokaryotes

After staining with the SYBR green II fluorescent dye, three clusters of heterotrophic prokaryotes were characterized by their different green fluorescence mean intensities (Fig. 2). Figure 5 shows the abundance of each heterotrophic prokaryote cluster at the surface, along with latitude. In the surface samples of the Kuroshio region the average concentrations of LNA, HNA and VHNA were, 8.71x10^5±3.8x10^5, 3.27x10^5±1.4x10^5 and 2.64x10^5±1.2x10^5 cells.cm^{-3}, respectively. In the Subtropical area the average concentrations of LNA, HNA and VHNA were 6.01x10^5±1.2x10^5, 2.97x10^5±1.4x10^5 and 1.84x10^5±6.4x10^4 cells.cm^{-3}, respectively. In the Transition zone the average concentrations of LNA, HNA and VHNA were 5.18x10^5±1.8x10^5, 4.38x10^5±1.6x10^5 and 1.15x10^5±6.2x10^5 cells.cm^{-3}, respectively. Despite the high variability between the concentrations along the north-south transect, the distribution of the three heterotrophic prokaryote groups was characterized by a common maximum at station 4 and a minimum at station 9. At station 4 the concentrations of LNA, HNA and VHNA were 1.39x10^6, 5.03x10^5 and 4.35x10^{5}cells.cm^{-3}, respectively. In contrast, the concentrations of LNA, HNA and VHNA at station 9 were 2.07x10^5, 1.6x10^5 and 5.07x10^{4}cells.cm^{-3}, respectively. To a lesser extent, high concentrations of LNA (9.13x10^{5}cells.cm^{-3}) and HNA (3.62x10^{5}cells.cm^{-3}) were identified at the northernmost station of the Kuroshio region (at station 1).

The vertical distributions of heterotrophic prokaryotes were also investigated along the transect (Fig. 6). As for surface, the vertical distributions of all heterotrophic prokaryote groups are characterized by lower cell concentrations at station 9. In this very station both

LNA and HNA concentrations are significantly lower than at the other stations (Kruskal wallis test, n = 90, P value < 0.05). The LNA cluster is numerically dominant in 99 % of the samples. The VHNA concentrations are lower than the HNA in 75 % of the samples. The contributions of each heterotrophic prokaryote cluster in terms of carbon biomass integrated between the surface and the 200 m depth to the total heterotrophic prokaryote carbon biomass (sum of the biomasses of the three heterotrophic prokaryote clusters) is shown in Fig. 7. LNA numerically dominated the carbon biomass from surface to the depth of 200 m (Sta. 5 to Sta. 12). The latitudinal contribution of the LNA cluster to the total heterotrophic prokaryotes in terms of carbon biomass varied from 47 % (Sta. 9) to 63 % (Sta. 6). Contribution of the HNA cluster is characterized by a low percentage at stations 5 and 6 (22 % and 16 %, respectively) and a near constant contribution between station 7 and the southernmost station 12 (33 ± 2 %; n=6). The contribution of the VHNA cluster was nearly constant from station 5 to 9 (19 ± 2 %; n=5). Then, it reached the lower values in the Transition zone (14 % at Sta. 10, 5 % at Sta.11 and 12 % at Sta.12).

Figure 8a displays the ratios of HNA/LNA concentration depending on depth. In the Kuroshio region, ratios are low and varied from 0.29 (Sta. 2) to 0.44 (Sta. 3). In the Subtropical gyre area, the ratios varied from 0.16 (Sta. 5, 70 m) to 0.82 (Sta. 7, 10 m). The higher ratios (up to 1.03 at Sta. 10, 10 m) were observed in the surface layer of the Transition zone. In the Transition zone and the Subtropical gyre area the higher ratios measured were found between the surface and 100 m. Figure 8b shows the ratio of VHNA/HNA concentrations depending on depth. In the Kuroshio region the ratio varied from 0.53 (Sta. 3) to 1.46 (Sta. 2). In the Subtropical gyre area, the ratio varied from 0.10 (Sta. 7, 58 m) to 1.93 (Sta. 9, 175 m). In the Transition zone the ratio varied from 0.10 (Sta. 12, 70 m) to 1.47 (Sta. 12, 180 m). The average of the VHNA/HNA ratio (0.37 ± 0.35) in the Transition zone was the lowest of the three sampled regions (0.78 ± 0.44 in the Subtropical gyre; 0.88 ± 0.41 in the Kuroshio region).

3.4 Statistical analysis

Results of the Principal Component Analysis (PCA) and the Redundance Analysis (RDA) are shown in Figs. 9 and 10, respectively. The correlation circle of the PCA, displays the first two principal components (PC1 and PC2) which accounted for 32.44 and 27.67 % of the total inertia, respectively. The third and fourth principal components are not shown due to the low inertia exhibited (11 and 8 % of the total inertia, respectively) and the lack of any

clear ecological understanding. Silicic acid, Chl *a*, VHNA and LNA where differentiated from temperature and salinity by PC1, while PC2 mainly differentiated depth, nitrate, and phosphate (negative coordinates) from the HNA clusters (positive coordinate). Using hierarchical classification the sampling depths were separated into six different clusters (Table 3 and Fig. 9.) Cluster 1, black dot, characterized all the stations located in the Kuroshio region. Cluster 2 samples were collected at the edge of the Subtropical gyre but also contained the deepest sample collected at station 9 (200 m), which was in the anticyclone eddy in the transition zone. All samples in Cluster 3 were collected below a depth of 125 m where nitrate and phosphate concentrations were higher than for surface samples. This cluster was defined as the deep layer group. Cluster 4 samples were collected in the center of the subtropical gyre (stations 7 and 8) where heterotrophic prokaryote concentrations were at their maximum in the seawater column. Cluster 5 represented the samples collected in the anticyclonic eddy where a marked salinity has been reported (Girault et al., 2013b). Located in the Transition zone, at the southernmost stations the sixth and last cluster group was characterized by the highest salinity and temperature values. This last cluster (blue dots in the Fig. 9a) is distinguished from the deep layer group (Cluster 3, green dots) by the low nutrient concentrations measured in the upper layer.

A redundancy analysis (Fig. 10) was then performed to find out how the measured environmental factors influenced the distribution of heterotrophic prokaryote subgroups sampled during the cruise. The cumulative percentage of all canonical eigenvalues indicated that 69.1 % of the observed heterotrophic cluster variations were explained by environmental factors. The first two axes of the RDA explained 38 and 24 % of the total variance, respectively. Monte-Carlo tests for these two axes were significant (P value < 0.05, using 999 permutations) and suggested that environmental parameters might be important in explaining heterotrophic prokaryote distribution. The first axis is negatively correlated with salinity and positively correlated with the LNA cluster. The second axis is negatively correlated with temperature and the HNA cluster and positively correlated with the VHNA cluster. RDA suggested two main correlations between the LNA cluster and the phytoplankton-related variables (Chl a and silicic acid) and the HNA cluster with the depth-related variables (nutrients such as nitrate and phosphate and depth).

To confirm and quantify these possible correlations 4 partial RDAs were also performed: one partial RDA using all the heterotrophic prokaryotes at once and one additional partial RDA for each heterotrophic prokaryote subgroup (LNA, HNA and VHNA). Results of the partial RDA performed on all the heterotrophic prokaryotes showed that among the six

environmental variables measured during the cruise, salinity and temperature statistically contribute for 24 and 7.5 % of the variation of the heterotrophic prokaryotes, respectively. To a lesser extent, phosphate alone explained 3.5 % of the variability, whereas Chl a, nitrate, depth and silicic acid explained only 1.8, 1.7, 1.7 and 0.86 %, respectively. The partial RDAs performed either on LNA, or HNA, or VHNA indicated that environmental parameters can explain 60, 55 and 27 % of the total variance, respectively (Table 4). Partial RDA results showed that the spatial related parameters alone can explain up to 31 % of the variation in the heterotrophic prokaryote distribution. The depth-related parameters explained between 6 and 8 % of the variance and finally the phytoplankton-related group explained a maximum 4 % of the variance in the LNA heterotrophic prokaryotes. As far as the HNA cluster is concerned, the joint variation of the spatial- and phytoplankton-related parameters explained 22 % of the variance.

4 Discussion

4.1 Relationship between the heterotrophic prokaryotes and phytoplankton along the oligotrophic gradient

The spatial distribution of the heterotrophic prokaryote clusters defined by flow cytometry can be discriminated into three main areas that correspond to different seawater masses: (i) the Kuroshio region, where the highest heterotrophic prokaryote concentrations were measured, (ii) the Subtropical gyre and (iii) the Transition zone both characterized by a high variability in the heterotrophic prokaryote concentrations in the seawater column (Figs. 1, 5 and 6). Separation between the Subtropical gyre and the Transition zone was made using the salinity front observed south of station 8 (Girault et al., 2013b). The hierarchical classification performed on the first two axes of the PCA, statistically confirmed this latitudinal pattern and also provided additional information on the relationships between the environmental parameters and specific mesoscale structures encountered during the cruise. Discrimination of six different clusters highlighted the complex assemblages of the mesoscale structures in the three main areas as previously reported in the NPSG area (Aoki et al., 2002) (Fig. 9). For example, stations located in the Transition zone were statistically discriminated into two clusters (Clusters 5 and 6) due to the high salinity and temperature values in the anticyclonic eddy (station 9). In addition to the latitudinal variations, vertical distribution is also important and this is taken into consideration with cluster 3. This cluster

grouped the deep layer samples which were characterized by higher nutrient concentrations than found in the upper layer (negative coordinates on PCA2). An interesting result obtained from the PCA and RDA, is that PC1 characterized both the silicic acid and Chl a concentrations. This result suggests a possible link between the abundance of phytoplankton and silicic acid concentrations. Concerning the large phytoplankton, evidence of Si depletion (<11 nmol.L^{-1}) associated with bloom of diatoms was previously reported in the Kuroshio current and highlighted that under specific conditions such as an eddy, large phytoplankton can be controlled in part by the availability of the silicic acid in this area (Hashihama et al., 2014). However, the effect of silicic acid on phytoplankton over a larger scale is unexpected, as the lowest concentrations of phosphate and nitrate have been reported in the euphotic layer of the western part of the NPSG area, and Si : N : P stoichiometry measured during the Tokyo–Palau cruise identified nitrogen and/or phosphorus to be potential limiting factors (Hashihama et al., 2009, 2014; Girault et al., 2013b). The nature of the control and the role of microorganisms with a smaller size, including small diazotrophs, on the silicic acid uptake are still controversial. Based on the nutrient uptake values measured in the NPSG area, relationship between the very high efficient uptake of silicic acid and silicified organisms was reported in Krause et al. (2012). This high efficiency of silicic acid uptake may explain in part the correlation between these two variables as observed both in the PCA and RDA despite the low concentrations of large silicified organisms measured in this area (Girault et al., 2013a). On the other hand, measurements of the Si-bioaccumulation in some strains of *Synechococcus* were reported in Baines et al. (2012), suggesting that some organisms without a Si-skeleton may also be involved in this silicic acid-Chl *a* correlation. In the Tokyo–Palau cruise, high *Synechococcus* concentrations were measured in the Subtropical gyre and in the Kuroshio regions and may lead to an unidentified Si pool in these areas. Finally, the availability of a Si pool may be in part promoted by the regeneration mechanism initiated from the marine bacterial assemblages (Bidle and Azam, 1999). The association of silicic acid and Chl *a* was proposed in this study to quantify the extent to which environmental parameters can explain the variation in heterotrophic prokaryotes. This approach seemed to be ecologically sound for the Tokyo–Palau cruise, as demonstrated by the partial RDA (silicic acid and Chl a were grouped together).

By using partial RDA analyses, the quantification of the effects of the environmental variables was in agreement with the PCA results. The hydrological parameters including temperature, salinity and to a lesser extent nutrients confirms the key role of the mesoscale

circulation. At the subgroup level LNA, HNA, and VHNA distributions appeared to be spatially different. This pattern is illustrated with the patchy distribution of the VHNA in comparison to the LNA and HNA distributions. With only 27 % of the variance explained, the distribution of VHNA is difficult to relate to the specific environmental parameters measured during the cruise, despite a non-negligible part of total variation explained by temperature and salinity (Table 4). The significant role of spatial-related variables is also observed in the LNA and HNA cluster distributions and matches well with the mesoscale circulation. “Pure” phytoplankton-related variables (Chl a, silicic acid) as a general control (bottom up) of the VHNA, HNA, and LNA distributions accounted only for a small fraction (1–4 %) of the explained variation. Indeed, in contrast to some recent investigations, this study suggests that Chl a and silicic acid variables are poorly correlated to the distribution of the various heterotrophic prokaryote subgroups (Sherr et al., 2006; Bouvier et al., 2007; Van Wambeke et al., 2011). However, when the phytoplankton-related variables were combined with spatial-related variables, the combination gave a negative loading for VHNA and LNA, while 22 % of the variance was calculated for the HNA. This may suggest that phytoplankton related variables are less important for VHNA and LNA than for HNA. This means that the variation in HNA is more likely to be spatial and phytoplankton dependent. The link between HNA and the spatial- and phytoplankton-related variables is not obvious in Fig. 9 because PCA cannot quantify the unique variation belonging to the specific variables. The partial RDA provided possible evidence and quantified that: (i) the LNA distribution is mainly explained by temperature and salinity and (ii) HNA distribution is mainly explained by an association of variables (temperature, salinity, Chl a and silicic acid) rather than a single environmental factor.

4.2 Diffusive nutrient fluxes and their biological relevance

Relationships between the vertical distribution of nutrients and ultraphytoplankton were investigated in a previous article (Girault et al., 2013b). Results pointed out that both phosphate and nitrate concentrations were particularly low in the upper layer of the ocean and characterized an oligotrophic environment combined with a complex assemblage of seawater masses. Calculation of Brunt-Väisäla buoyancy frequencies confirmed the well stratified structure observed along the transect, especially at stations 10 and 11 where the higher values of N^2 were found. Contrasting to some other oligotrophic areas the depth receiving 1 % of the irradiance in surface (used to define the euphotic layer) was not coupled with the thermocline, suggesting that a part of the organic material could be

transported below the euphotic layer (by vertical migration of organisms for instance). In these low nutrient conditions, theoretical calculation of nutrient supplies from the mixed layer was investigated in order to estimate the influence of these nutrient supplies in the upper mixed layer (Tables 1 and 2). The results obtained should obviously be taken with caution, especially for nitrates due to the importance of diazotrophy as previously reported and to episodic dust deposition not negligible in the NPSG (Wilson, 2003; Kitajima et al., 2009; Maki et al., 2011). However, results of the phosphate and nitrogen diffuse fluxes were in agreement with the value reported in oligotrophic conditions (Gasol et al., 2009). Silicic acid diffuse fluxes were also in the range of values reported by Painter et al., (2014). Negative diffuse fluxes of phosphate observed at stations 5 and 6 resulted from the variation of phosphate concentration in the mixed layer and the depth of the phosphacline (found at ~200 m depths). The oscillation of positive and negative values in phosphate-depleted condition also pointed out the approximation linked to the limit of detection of the phosphate concentration (3 nM) in the oligotrophic upper layer. The comparison between the phosphate or silicic acid fluxes and the mixed layer integrated concentration of nutrients suggested that the daily diffuse fluxes were of minor importance to resupply nutrients to the surface Ocean. This result is coherent with the oligotrophic conditions observed during the cruise and emphasized the important role of the microbial loop to sustain the growth of organisms in the western part of the NPSG.

The particular high gradient in nutrients observed between 100 m and 155 m depth at station 8 matched very well with the possible presence of the subtropical counter current, STCC (Sta. 100 m to 130 m), as reported in Girault et al., (2013b). Despites no noticeable pattern of variation of buoyancy frequency at these depths, nutrient gradients clearly indicated two zones of high gradients separated by a layer of lower or null gradient. Interestingly, the depths with high nutrient gradients were similar for silicic acid and phosphates but higher nitrate gradients were located just beneath this layer. This result suggested that utilization of nitrate differed from phosphates and silicic acid in the vicinity of the STCC layer. In terms of nitrate daily flux related to the standing pool, an anomalous percentage of 432% was evidenced suggesting that diffusive role of nitrates linked to the STCC was particularly important. This anomalous percentage was the result of two mechanisms *i*) a nitrate-depletion in the mixed layer and *ii)* the depth of the nitracline corresponded to the depth of the thermocline. Association of nitracline with thermocline mathematically maximized the daily flux related to the standing pool and lead to this high percentage at station 8. Although, Figure 6 did not evidence particular distribution of

heterotrophic prokaryotes close to the STCC layer, integrated heterotrophic prokaryote abundance and carbon biomass of HNA in the Subtropical gyre area were maximum at station 8 (Fig. 7). This result is also observed with the ultraphytoplankton distribution where high concentrations were also found at this station (Girault et al., 2013b). Relationships between the STCC and microbial food web *via* the nutrient fluxes appeared to be an important mechanism to sustain the ecosystem in the Subtropical pacific gyre area. Although the statistical analyses were performed on the entire data set, RDA results tend to confirm and emphasize this relationship between the variance of HNA distribution, phytoplankton distribution and depth related parameters (Table 2).

4.3 The role of nutrients in the distribution of HNA and LNA

The partial RDA showed that the "pure" depth-related variables explained between 6 and 8 % of the total heterotrophic prokaryotes variance. These percentages are low but the sum of their joint effect (including the depth-related variables) can explain more than 26 % of the total variation in the LNA distribution. Differences in nutrient utilisation and requirements could also lead to different heterotrophic prokaryote distributions and a possible discrimination of certain organisms subject to the oligotrophic gradient. These variations can in part be observed thanks to the ratios of the abundances of the various clusters (Fig. 8). Figure 8 shows two opposite relationships between the nucleic acid content of the heterotrophic prokaryotes and the spatial distribution. Considering the VHNA/HNA ratio, a northward increase of the ratio was found in the upper layer (from the surface to 100 m) and suggested that these microorganisms with a very high nucleic acid content are outcompeted by the HNA prokaryotes in the most oligotrophic region (Transition zone). It should be noted that the relationship between the VHNA and HNA appeared to be rather centered on the boundary between the Transition zone and the Subtropical gyre areas, and not related to a continuous modification of the ratio along the gradient (average and standard deviation of VHNA/HNA ratio in the Kuroshio region are close to the ones in the Subtropical gyre area). In contrast, Figure 8a shows that HNA/LNA ratio increased from the northernmost station 1 to the southward station 12 in the upper layer (from the surface to 100 m), especially from station 6. In addition, a decrease in the HNA/LNA ratio was found below 100 m at station 7 in the Subtropical gyre area through to the Transition zone. In opposition to other cruises conducted in oligotrophic conditions, the Tokyo–Palau cruise demonstrated a latitudinal gradient in VHNA, HNA and LNA concentrations in the upper layer and from the surface to the deep layer (Van Wanbeke et al., 2011). Nutrient data

displayed in Fig. 6 (Girault et al., 2013b) showed that both phosphate and nitrate concentrations decreased between stations 6 and 7 but were measured in high concentrations under the thermocline. From the perspective of nutrients these results suggest that LNA is less abundant than HNA under low phosphate and nitrate conditions. This is in contrast with the hypothesis proposed for severely P-limited environments which suggests that inorganic phosphorus can exert more severe physiological constraints on the growth of HNA than LNA (Nishimura et al., 2005; Wang et al., 2007). However, it is important to note that both LNA and HNA clusters are likely to include different strains of microorganisms including species adapted to the warm, which have been shown to have lower minimal P cell quotas (Hall et al., 2008). The link between these warm-adapted species and the nucleic acid content is still unclear and depends on the type of environment studied. For example, the warm-adapted species of LNA were expected to have an advantage over cells with high nucleic acid content (HNA) in the warm resource limited environment of the Mediterranean Sea (Van Wanbeke et al., 2011). In contrast, the work of Andrade et al. (2007) found that LNA accounted for the high proportion of cells in cold and "nutrient rich" waters, whereas cells with higher HNA concentrations were prominent in the oligotrophic high temperature regions of the Southwest Atlantic Ocean. According to Andrade et al. (2007), the variation in the HNA/LNA ratio observed suggests that low nutrient conditions favour HNA cells over LNA cells. This result along with the statistical analyses performed in this study may suggest that HNA species are more warm-adapted than LNA in the Subtropical gyre and Transition zone. Decrease of the VHNA/HNA ratio also suggests that the numerically dominant species with high nucleic acid content (HNA) might be more warm-adapted than the cells with the highest nucleic acid content (VHNA). These contrasting results highlight the complex and non linear link between the cell nucleic acid contents and the various ecological meanings as reported in Bouvier et al., (2007) and Van Wanbeke et al., (2009).

4.4 Distribution of the heterotrophic prokaryotes and eddies

During the Tokyo–Palau cruise the transect crossed a cold core cyclonic eddy near station 3 and a warm core cyclonic eddy at station 9. Cyclonic eddies usually enhance biological activities as reported by the measurements of carbon fixation, nutrient uptake, and oxygen production (Bidigare et al., 2003). At station 3, the pumping effect initiated by the cyclonic eddy was seen by recording the nutrient ratio and identifying the microphytoplankton taxonomy (Girault et al., 2013a, b). The high concentration of Chl a measured at station 3

and the numerical dominance of large phytoplankton agreed with the description of cold core cyclonic eddy event (Vaillencourt et al., 2003). A high concentration of heterotrophic prokaryotes was found at the edge of the cyclonic eddy (Sta. 4). The effect of the eddy on the similar concentrations of heterotrophic prokaryotes were measured at stations 2 and 3. In oligotrophic conditions, environmental factors controlling the distribution of the heterotrophic prokaryotes were compared in two extreme cases: the stations located under the influence of the eddy and the ones outside its influence (Baltar et al., 2010). However, few investigations target the distribution of heterotrophic prokaryotes along the spatial oligotrophic gradient (Thyssen et al., 2005) or take into account the age of eddy (Sweeney et al., 2003; Rii et al., 2007). With three stations only (stations 2, 3, 4), a snapshot of the eddy effects was presented and it remained difficult, not to say impossible, to describe the local effect of the eddy. However, by using satellite data and daily surface currents of the bulletin of the Japanese coast guard, it was possible to detect that the creation of the eddy structure was linked to the instability in the meander of the Kuroshio Current between 9 and 12 July 2010. This phenomenon has been commonly observed in this area (e.g. 17 April 2012; 14 May 2013) and its lifespan is usually about a month. In comparison, the sea surface current map suggested that the mesoscale structure observed during the cruise was older than six months. On the basis of the “closed” model proposed for an eddy, a six month old cyclonic eddy is associated with its decay phase, where intense blooms can be observed but which lack significant diatom abundance (Seki et al., 2001). During the cruise, the highest abundance of microphytoplankton was observed at station 3, suggesting that the classical biogeochemical properties normally associated with an eddy (i.e. single nutrient pulse, “closed system”) were not apparent in the cyclonic eddy encountered during the Tokyo–Palau cruise. This phenomenon has also been observed in other oligotrophic areas (Seki et al., 2001; Bidigare et al., 2003; Landry et al., 2008). According to Nencioli et al. (2008), the association of a horizontal translation gradient with multiple nutrient inputs might explain the variability in organisms between stations 2, 3, and 4. Indeed, the cold core of the cyclonic eddy moved to the north-west between December and the sampling time of the cruise. Station 4 therefore is the first station to be influenced by the eddy, the center of cyclonic eddy then moved towards station 3, but did not reach station 2 located in the vicinity of the Kuroshio Current. The path of the cold core cyclonic eddy could explain the possible decrease in the nutrient uptake from the bottom layer at station 4 and lead to an oligotrophic system dominated by regeneration processes. The high abundance of heterotrophic prokaryotes measured at the edge of the cyclonic eddy could be explained by

the high activity in the microbial loop. This difference in heterotrophic prokaryote abundance between the center and the edge of the eddy may be due to a more efficient vertical exchange of seawater masses which has been reported at the periphery of some eddies rather than at the center of them (Stapleton et al., 2002; Klein and Lapeyre, 2009). Similarly, the numerical dominance of Synechococcus, observed only once in the surface samples during the cruise, may explain the change in trophic conditions (Girault et al., 2013b).

The frontal structures observed between the Subtropical gyre and the Transition zone are usually defined by an accumulation zone for organic matter and an area of high heterotrophic prokaryote abundance is found (Arístegui and Montero, 2005; Baltar et al., 2009; Lasternas et al., 2013). However, the anticyclonic eddy at station 9 is characterized by the lowest concentrations of heterotrophic prokaryote clusters found during the cruise. The low concentrations of the dominant LNA cluster was also observable in terms of integrated carbon biomass, and highlighted the response of each cluster to the change of environmental conditions, such as the salinity front (Fig. 7), Among the environmental variables, low nutrient concentrations are expected to be one factor controlling the specific distribution of heterotrophic prokaryote clusters (Girault et al., 2013b). The partial RDA suggests that the spatial related variables are the most important, followed by the “pure” depth-related variables which explained between 6 and 8 % of the total variation in the heterotrophic prokaryote cluster abundances. The low difference in percentages between LNA, HNA, and VHNA clusters was in agreement with the constant numerically dominant group found between the surface and 160 m. This result suggested that the anticyclonic eddy did not enhance nor limit one particular heterotrophic prokaryote cluster in the upper layer (Fig. 6). However, below 160 m a high increase in VHNA and LNA abundance was measured compared to HNA. This result is uncommon in the meso- and bathypelagic zones of oligotrophic areas where the concentration of HNA and LNA heterotrophic prokaryotes decreased significantly with depth (Van Wambeke et al., 2011; Yamada et al., 2012). The increase in nutrient concentrations associated with the sloppy feeding mechanism initiated by the concentration of VHNA may partially lead to the high abundance of LNA observed at the bottom of the euphotic layer (Thyssen et al., 2005).

5 Conclusions

This study along a 2300 km transect in the North Pacific subtropical gyre area during a

strong La Niña condition showed that the heterotrophic prokaryote distribution is correlated with three different seawater masses identified as (i) the Kuroshio, (ii) the Subtropical gyre and (iii) the Transition zone. A latitudinal increase in the HNA/LNA ratio was found along the equatorward oligotrophic gradient and suggested different relationships between the various heterotrophic clusters and the environmental variables measured in situ during the cruise. The statistical analyses highlighted that the majority of the heterotrophic prokaryote distribution is explained by temperature and salinity. Nutrients and phytoplankton-related variables had different influences depending on the LNA, HNA and VHNA clusters. LNA distribution is mainly correlated with temperature and salinity while HNA distribution is mainly explained by an association of variables (temperature, salinity, Chl a and silicic acid). During the cruise, two eddies (one cyclonic and one anticyclonic) were crossed. The vertical distributions of LNA, HNA and VHNA were investigated. Based on the current surface map and the microorganism distribution, it is reasonable to form the hypothesis that the high concentration of heterotrophic prokaryotes observed at station 4 was linked to the path of the cold cyclonic eddy core. In contrast, in the warm core of the anticyclonic eddy, lower heterotrophic prokaryote concentrations are suggested to be linked to the low nutrient concentrations. All the results described in this study highlight the high variability of each heterotrophic prokaryote cluster defined by their nucleic acid content (LNA, HNA, and VHNA) with regard to the mesoscale structures and the oligotrophic gradient observed in situ within the area of the North Pacific subtropical gyre.

Acknowledgements

We thank Captain Akira Noda, crew members of the RT/V Shinyo maru of Tokyo University of Marine Science and Technology, (TUMSAT) for their cooperation at sea. We appreciated the English correction of the manuscript made by Tracy L. Bentley. We thank Yuta Nakagawa and Shinko Kinouchi for their help during the cruise. We are grateful to the PRECYM Flow Cytometry Platform of the Mediterranean Institute of Ocenaography (MIO) for the flow cytometry analyses. We also thank the Société franco-japonaise d'Océanographie for its support in shipping the samples from Japan to France.

References

Andrade, L., Gonzale,z A. M., Rezende, C. E., Suzuki, M., Valentin, J. L., and Paranhos, R.: Distribution of HNA and LNA bacterial groups in the Southwest Atlantic Ocean, Braz. J. Microbiol., 38, 330-336, 2007.

Aoki, Y., Suga, T., and Hanawa, K.: Subsurface subtropical fronts of the North Pacific as inherent boundaries in the ventilated thermocline, J. Phys. Oceanogr., 32, 2299–2311, 2002.

Arístegui, J. and Montero, M. F.: Temporal and spatial changes in plankton respiration and biomass in the Canary Islands region: the effect of mesoscale variability, J. Mar. Syst., 54, 65–82, 2005.

Baines, S. B., Twining, B. S., Brzezinski, M. A., and Nelson, D. M.: An unexpected role for picocyanobacteria in the marine silicon cycle, Nature Geosci., 5, 886–891, 2012.

Baltar, F., Arístegui, J., Montero, M. F., Espino, M., Gasol, J. M., and Herndl, G. J.: Mesoscale variability modulates seasonal changes in the trophic structure of nano- and picoplankton communities across the NW Africa-Canary Islands transition zone, Prog. Oceanogr., 83, 180–188, 2009.

Baltar, F., Arístegui, J., Gasol, J. M., Lekunberri, I., and Herndl, G. J.: Mesoscale eddies: hotspots of prokaryotic activity and differential community structure in the ocean, ISME J., 4, 975–988, 2010.

Bidigare, R. R., Benitez-Nelson, C., Leonard, C. L., Quay, P. D., Parsons, M. L., Foley, D. G., and Seki, M. P.: Influence of a cyclonic eddy on microheterotroph biomass and carbon export in the Lee of Hawaii, Geophys. Res. Letters, 30, 51, 1-4, 2003.

Bidle, K. D. and Azam F.: Accelerated dissolution of diatom silica by marine bacterial assemblages, Nature, 397, 508-512, 1999.

Bouvier, T, del Giorgio, P. A, and Gasol, J. M.: A comparative study of the cytometric characteristics of high and low nucleic–acid bacterioplankton cells from different aquatic ecosystems, Environ. Microbiol., 9, 2050–2066, 2007.

Caron, D. A., Dam, H. G., Kremer, P., Lessard, E. J., Madin, L. P., Malone, T. C., Napp, J. M., Peele, E. R., Roman, M. R., and Youngbluth, M. J.: The contribution of microorganisms to partic- ulate carbon and nitrogen in surface waters of the Sargasso Sea near Bermuda, Deep-Sea Res. I, 42, 943–972, 1995.

Currie, D. J. and Kalff, J.: Can bacteria outcompete phytoplankton for phosphorus? A chemostat test, Microb. Ecol., 10, 205-216, 1984.

Del Grosso, V. A.: New equation for the speed of sound in natural waters with comparisons to other equations, J. Acoust. Soc. Am. 56, 1084–1091, 1974.

Duhamel, S., Dyhrman, S. T., and Karl, D. M.: Alkaline phosphatase activity and regulation in the North Pacific Subtropical Gyre, Limnol. Oceanogr., 55, 1414–1425, 2010.

Emerson, S., Quay, P. D., Stump, C., Wilbur, D., and Schudlich, R.: Chemical tracers of productivity and respiration in the subtropical Pacific Ocean, J., Geophys., Res., 100, 15873-15887, 1995.

Garside, C.: A chemiluminescent technique for the determination of nanomolar concentrations of nitrate and nitrite in seawater, Mar. Chem., 11, 159–167, 1982.

Gasol J. M., Zweifel, U. L., Peters, F., Fuhrman, J. A., and Hågström, A.: Significance of size and nucleic acid content heterogeneity as measured by flow cytometry in natural planktonic bacteria, App. Environ. Microbiol., 65, 4475–4483, 1999.

Gasol J. M., Vázquez-Domínguez, E., Vaqué, D., Agustí, S., and Duarte, C. M.: Bacterial activity and diffuse nutrient supply in the oligotrophic central Atlantic Ocean, Aquat. Microb. Ecol., 56, 1-12, 2009.

Girault, M., Arakawa, H., and Hashihama, F.: Phosphorus stress of microphytoplankton community in the western subtropical North Pacific, J. Plankton Res., 35, 146-157, 2013a.

Girault, M., Arakawa, H., Barani, A., Ceccaldi, H. J., Hashihama, F., Kinouchi, S., and Grégori, G.: Distribution of ultraphytoplankton in the western part of the North Pacific subtropical gyre during a strong La Niña condition: relationship with the hydrological conditions, Biogeosciences, 10, 5947-5965, 2013b.

Grégori, G., Denis, M., Lefevre, D., and Romano, J. C.: Viability of heterotrophic bacteria in the Bay of Marseilles, C. R. Biol., 326, 739-750, 2003a.

Grégori G., Denis, M., Sgorbati, S., and Citterio, S.: Resolution of viable and membrane-compromised free bacteria in aquatic environments by flow cytometry, Curr. Protoc. Cytom., 23, 11.15.1–11.15.7, 2003b.

Grégori G., Citterio, S., Ghiani A., Labra, M., Sgorbati, S., Brown, S., Denis, M.: Resolution of viable and membrane compromised bacteria in fresh and marine waters based on

analytical flow cytometry and nucleic acid double staining, Appl. Environ. Microbiol., 67, 4662-4670, 2001.

Hall, E. K., Neuhauser, C., and Cotner, J.: toward a mechanistic understanding of how natural bacterial communities respond to changes in teperature in aquatic ecosystems, ISME, 2, 471–481, 2008.

Hashihama, F., Furuya, K., Kitajima, S., Takeda, S., Takemura, T., and Kanda, J.: Macro-scale exhaustion of surface phosphate by dinitrogen fixation in the western North Pacific, Geoph. Res. Lett., 36, L03610, doi:10.1029/2008GL036866, 2009.

Hashihama, F. and Kanda, J.: Automated colorimetric determination of trace silicic acid in seawater by gas-segmented continuous flow analysis with a liquid waveguide capillary cell, La Mer, 47, 119–127, 2010.

Hashihama, F., Kanda, J., Maeda, Y., Ogawa, H., and Furuya, K.: Selective depressions of surface silicic acid within cyclonic mesoscale eddies in the oligotrophic western North Pacific, Deep-Sea Res. PT I, 90, 115-124, 2014.

Kataoka, T., Hodoki, Y., Suzuki, K., Saito, H., Higashi, S.: Tempo-spatial patterns of bacterial community composition in the western North Pacific Ocean, J. Marine Syst., 77, 197-207, 2009.

Kitajima, S., Furuya, K., Hashihama, F., Takeda, S., and Kanda, J.: Latitudinal distribution of diazotrophs and their nitrogen fixation in the tropical and subtropical western North Pacific, Limnol. Oceanogr., 54, 537–547, 2009.

King, B., Stone , M., Zhang, H. P., Gerkema, T., Marder, M., Scott, R. B. and Swinney, H. L.: Buoyancy frequency profiles and internal semidiurnal tide turning depths in the oceans, J. Geophys. Res., 117, C04008, DOI:10.1029/2011JC007681, 2012.

King, F. D., and Devol, A. H.: Estimates of vertical eddy diffusion through the thermocline from phytoplankton nitrate uptake rates in the mixed layer of the estern tropical Pacific., Limnol, Oceanogr., 24, 645-651, 1979.

Klein, P. and Lapeyre G.: The oceanic vertical pump induced by mesoscale and submesoscale turbulence, Annu. Rev. Mar. Sci., 1, 351-375, 2009.

Kobari, T., Hijiya, K., Minowa, M., and Kitamura, M.: Depth distribution, biomass and taxonomic composition of subtropical microbial community in southwestern Japan, South Pacific Studies, 32, 31-43, 2011.

Krause, J. W., Brzezinski, M. A., Villareal, T. A., and Wilson, C.: Increased kinetic efficiency for silicic acid uptake as a driver of summer diatom blooms in the North Pacific subtropical gyre, Limnol. Oceanogr., 57, 1084-1098, 2012.

Landry, M. R., Brown, S. L., Rii, Y. M., Selph, K. E., Bidigare, R.R., Yang E.J., and Simmons, M. P.: Depth-stratified phytoplankton dynamics in Cyclone Opal, a subtropical mesoscale eddy, Deep-Sea Res. PT II, 56, 1348-1359, 2008.

Lasternas, S., Piedeleu, M., Sangrà, P., Duarte, C. M., and Agustí, S.: Forcing of dissolved organic carbon release by phytoplankton by anticyclonic mesoscale eddies in the subtropical NE Atlantic Ocean, Biogeosciences, 10, 2129-2143, 2013.

Lebaron, P., Parthuisot, N., and Catala, P.: Comparison of blue nucleic acid dyes for flow cytometric enumeration of bacteria in aquatic systems, Appl. Environ. Microbiol., 64, 1725-1730, 1998.

Lebaron, P., Servais, P., Agogue, H., Courties, C., and Joux, F.: Does the high nucleic acid content of individual bacterial cells allow us to discriminate between active cells and inactive cells in aquatic systems?, Appl. Environ. Microbiol. 67, 1775–1782, 2001.

Ledwell, J. R., Watson, A. J., and Laws, C. S.: Mixing of a tracer in the pycnocline, J. Geophys. Res., 103, 21499–21529, 1998.

Ledwell, J. R., Mc Gillicuddy Jr., D. J., and Anderson, L. A.: Nutrient flux into an intense deep chlorophyll layer in a mode-water eddy, Deep-Sea Res. Pt. II, 55, 1139–1160, 2008.

Li, Y.-H., Peng, T.-H., Broecker, W. S., and Göte Östlund H.: The average vertical mixing coefficient for the oceanic thermocline, Tellus, 36B, 212-217, 1984.

Lipkovich, L. I and Smith, E. P.: Biplot and singular value decomposition macros for Excel®, J. Stat. Softw., 7, 1-15, 2002.

Liu, Q.: Variation partitioning by partial redundancy analysis (RDA), Environmetrics, 8, 75-85, 1997.

Maki, T., Ishikawa, A., Kobayashi, F., Kakikawa, M., Aoki, K., Mastunaga, T., Hasegawa H., and Iwasaka, Y.: Effects of Asian dust (KOSA) deposition event on bacterial and microalgal communities in the Pacific Ocean, Asian Journal of Atmospheric Environment, 5, 157-163, 2011.

Marie, D., Brussaard, C. P. D., Thyrhaug, R., Bratbak, G., and Vaulot, D.: Enumeration of

marine viruses in culture and natural samples by flow cytometry, Appl. Environ. Microbiol., 65, 45–52, 1999.

Mitbavkar, S., Saino, T., Horimoto, N., Kanda, J., and Ishimaru T.: Role of environment and hydrography in determining the picoplankton community structure of Sagami Bay, Japan, J. Oceanogr., 65, 195-208, 2009.

Nencioli, F., Dickey, T. D., Kuwahara V. S., Black W., Rii, Y. M., and Bidigare, R. R.: Physical dynamics and biological implications of a mesoscale cyclonic eddy in the Lee of Hawaii: Cyclone Opal observations during E-Flux III, Deep-Sea Res. PT II, 55, 1252–1274, 2008.

Nishimura, Y., Kim, C., and Nagata, T.: Vertical and seasonal variations of bacterioplankton subgroups with different nucleic acid contents: possible regulation by phosphorus, Appl. Environ. Microbiol., 71, 5828-5836, 2005.

Painter, S. C., Henson, S. A., Forryan, A., Steigenberger, S., Klar, J., Stinchcombe, M. C., Rogan, N., Baker, A. R., Achterberg, E. P., and Moore, C. M.: An assessment of the vertical diffusive flux of iron and other nutrients to the surface waters of the subpolar North Atlantic Ocean, Biogeosciences, 11, 2113-2130, 2014.

Pearson, K.: On lines and planes of closest fit to systems of points in space, Philos. Mag., 2, 559–572, 1901.

Rii, Y. M., Brown Susan, L., Nencioli, F., Kuwahara, V., Dickey, T., Karl D. M., and Bidigare, R. R.: The transient oasis: Nutrient-phytoplankton dynamics and particle export in Hawaiian lee cyclones, Deep-Sea Res. PT II, 55, 1275–1290, 2008.

Rooth, C., and Ostlund H. G.: Penetration of tritium into the Atlantic thermocline, Deep-Sea Res. 19, 481-492, 1972.

Seki, M. P., Polovina, J. J., Brainard, R. E., Bidigare, R. R., Leonard, C. L., and Foley, D. G.: Biological enhancement at cyclonic eddies tracked with goes thermal imagery in hawaiian waters, Geophys. Res. Lett., 28, 1583–1586, 2001.

Sekine, Y. and Miyamoto, S.: Influence of Kuroshio flow on the horizontal distribution of north Pacific intermediate water in the Shikoku basin, J. Oceanogr., 58, 611–616, 2002.

Sherr, B., Sherr, E., and Longnecker, K.: distribution of bacterial abundance and cell-specific nucleic acid content in the Northeast Pacific Ocean, Deep-Sea Res. PT I, 53, 713–725, 2006.

Sieracki, M. E., Haugen, E. M., and Cucci, T. L.: Overestimation of heterotrophic bacteria in the Sargasso Sea: direct evidence by flow and imaging cytometry. Deep Sea Res. PT I, 42, 1399–1409, 1995.

Sprintall, J., and Roemmich, D., Characterizing the structure of the surface layer in the Pacific Ocean, J. Geophys. Res., 104, 23297-23311, 1999.

Stapleton, N. R., Aicken, W. T., Dovey, P. R., and Scott, J. C.: The use of radar altimeter data in combination with other satellitesensors for routine monitoring of the ocean: case study of the northern Arabian sea and Gulf of Guam, Can. J. Remote Sens., 28, 567-572, 2002.

Suzuki, R. and Ishimaru, T.: An improved method for the determination of phytoplankton chlorophyll using N,N-Dimethylformamide, J. Oceanogr. Soc. Japan, 46, 190–194, 1990.

Sweeney, E. N., McGillicuddy, D. J., and Buesseler, K. O.: Bio- geochemical impacts due to mesoscale eddy activity in the sargasso sea as measured at the bermuda atlantic time-series study (BATS), Deep Sea Res. PT II, 50, 3017–3039, 2003.

Thingstad T. F., Zweifel, U. L., and Assoulzadegan, F. R.: P-limitation of heterotrophic bacteria and phytoplankton in the north- west Mediterranean, Limnol. Oceanogr. 43, 88–94, 1998.

Thyssen, M., Lefèvre, D., Caniaux, G., Ras, J., Fernández, C. I., and Denis, M.: Spatial distribution of heterotrophic bacteria in the northeast Atlantic (POMME study area) during spring 2001, J. Geophys Res., 110, C07S16, DOI: 10.1029/2004JC002670, 2005.

Vadstein, O.: Evaluation of competitive ability of two heterotrophic planktonic bacteria under phosphorus limitation, Aquatic Microb. Ecol., 14, 119-127, 1998.

Vaillancourt, R. D., Marra, J., Seki, M. P., Parsons, M. L., and Bidigare, R. R.: Impact of a cyclonic eddy on phytoplankton community structure and photosynthetic competency in the subtropical North Pacific Ocean, Deep Sea Res. PT I, 50, 829–847, 2003.

Van Scoy, K. A., and Kelley, D. E.: Inferring vertical diffusivity from two decades of tritium penetration, EOS, Trans. AGU., 77, Ocean Sci. Meet. Suppl. OS40, 1996.

Van Wambeke, F., Ghiglione, J.-F., Nedoma, J., Mével, G., and Raimbault, P.: Bottom up effects on bacterioplankton growth and composition during summer-autumn transition in the open NW Mediterranean Sea, Biogeosciences, 6, 705-720, doi:10.5194/bg-6-705-2009, 2009.

Van Wambeke, F., Catala, P., Pujo-Pay, M., and Lebaron, P.: Vertical and longitudinal gradients in HNA-LNA cell abundances and cytometric characteristics in the Mediterranean Sea, Biogeosciences, 8, 1853-1863, DOI: 10.5194/bg-8-1853-2011, 2011.

Vernet, M. and Lorenzen, C. J.: The presence of chlorophyll *b* and the estimation of phaeopigments in marine phytoplankton. J. Plankton Res., 9, 265-265, 1987.

Wang, H., Smith, H. L., Kuang, Y., and Elser, J. J.: Dynamics of stoichimotric bacteria-algae interactions in the epilemnion, Siam J. Appl. Math., 68, 503–522, 2007.

White, W., and Bernstein, R.: Large-scale vertical eddy diffusion in the main pycnocline of the central North Pacific, J. Phys., Oceanogr., 11, 434-441, 1981.

Wilson, C., Late Summer chlorophyll blooms in the oligotrophic North Pacific Subtropical Gyre, Geophys. Res. Lett., 30, 1942, doi:10.1029/2003GL017770, 2003.

Yamada N., Fukuda, H., Ogawa, H., Saito, H., and Suzumura, M.: Heterotrophic bacterial production and extracellular enzymatic activity in sinking particulate matter in the western North Pacific Ocean, Front. Microbiol., 3, 379, DOI: 10.3389/fmicb.2012.00379, 2012.

Zubkov, M. V., Fuchs, B. M., Burkill, P. H., and Amann, R.: Comparison of cellular and biomass specific activities of dominant bacterioplankton groups in stratified waters of the Celtic Sea, Appl. Environ. Microbiol., 67, 5210–5218, 2001.

Table 1. Literature estimates of vertical turbulent diffusivity rates obtained using different methods in the oligotrophic condition. *na* indicates information not mentioned.

Domain	Location	Depth (m)	Diffusivity ($cm^2.s^{-1}$)	Reference
North Pacific Subtropical Gyre	22°N-158°W	300-500	0.1-0.5	(Christian and Lewis, 1997)
	35–44°N, 150–170°W	*na*	0.2-0.4	(White and Berstein, 1981)
	10°N-40°N	0-1000	0.3	(Van Scoy and Kelley, 1996)
	22°N-158°W	*Euphotic*	1-2	(Emerson *et al.*, 1995)
Pacific Ocean	20°S-20°N	125	0.5	(Li *et al.*, 1984)
	20°N-60°N	100	1.8	(Li *et al.*, 1984)
Tropical North Pacific Ocean	5°N-10°N, 90°E	*na*	0.05-0.16	(King and Devol, 1979)
	10°N-15°N, 85°E	*na*	0.44-1.10	(King and Devol, 1979)
Subtropical North Atlantic	25°N, 28°W	300	0.12-0.17	(Ledwell *et al.*, 1998)
	28.5°N, 23°W	100-400	0.37	(Lewis *et al.*, 1986)
	31°N, 66°W	<100	0.35	(Ledwell *et al.*, 2008)

Table 2. Phosphate, nitrate and silicic acid diffusive fluxes into the surface mixed layer and the importance of supply term relative to the standing pool size.

Station	Latitude	Mixed layer depth (m)	Phosphate flux ($\mu mol.m^{-2}.d^{-1}$)	Daily diffusive supply relative to pool (%)	Nitrate flux ($\mu mol.m^{-2}.d^{-1}$)	Daily diffusive supply relative to pool (%)	Silicic acid flux ($\mu mol.m^{-2}.d^{-1}$)	Daily diffusive supply relative to pool (%)
5	28.98	141	-0.52	-0.01	3.63	0.01	2.25	0.002
6	27.16	136	-1.34	-0.03	12.88	0.04	54.09	0.03
7	24.83	109	9.43	0.69	0	0	142.21	0.21
8	22.83	101	7.78	0.76	81.3	432	351.36	0.39
9	20.78	140	6.48	0.68	13.91	5.7	571.1	0.48
10	19.98	95	1.38	0.16	0	0	0.006	0.01

Table 3. List of observations from stations 1 to 11 and their classification into six clusters according to the principal component analysis (PCA).

PCA Cluster	Observations	Latitude (°N)	Station	Depth (m)
1	1	33.6	1	0
1	2	33	2	0
1	3	31.6	3	0
1	4	31	4	0
2	5,6,7,8,9,10,11,12,13	28.6	5	0,40,60,70,78,80,100,120,140
2	15,16,17,18,19,20,21,22,23	27.1	6	0,25,60,75,80,90,100,115,125
2	32,33,34	24.5	7	75,90,101
2	40,41	22.5	8	110,125
2	55	20.5	9	200
3	14	28.6	5	160
3	24	27.1	6	150
3	42,43,44	22.5	8	135,150,165
3	54	20.5	9	160
3	61	19.6	10	125
4	25,26,27,28,29,30,31	24.5	7	0,10,25,40,58,59,60
4	35,36,37,38,39	22.5	8	0,25,50,75,95
5	45,46,47,48,49,50,51,52,53	20.78	9	0,25,50,75,100,120,130,140
5	59,60,62	19.6	10	75,100,150
6	56,57,58	19.6	10	0,25,50
6	63,64,65,66	17.2	11	0,30,45,60

Table 4. Partial redundancy analysis performed on each heterotrophic prokaryote cluster optically resolved by flow cytometry: low nucleic acid content (LNA), high nucleic acid content (HNA) and very high nucleic acid content (VHNA). According to the PCA results, Chl *a* and silicic acid are the phytoplankton-related variables. Temperature and salinity are the spatial-related variables. Nitrate, phosphate and depth are the depth-related variables. Negative values characterized the lack of any correlation between heterotrophic prokaryote clusters and the variables tested.

		LNA	HNA	VHNA
Total explained variance		60%	55%	27%
Joint variation	Phytoplankton-related and spatial- and depth-related	6%	-1%	-1%
Partial joint variation	Spatial-related and phytoplankton-related	-1%	22%	-4%
	Spatial- and depth-related	9%	1%	5%
	Depth-related and phytoplankton-related	3%	1%	0%
Unique variation	Phytoplankton-related	4%	1%	1%
	Depth-related	8%	8%	6%
	Spatial-related	31%	23%	20%

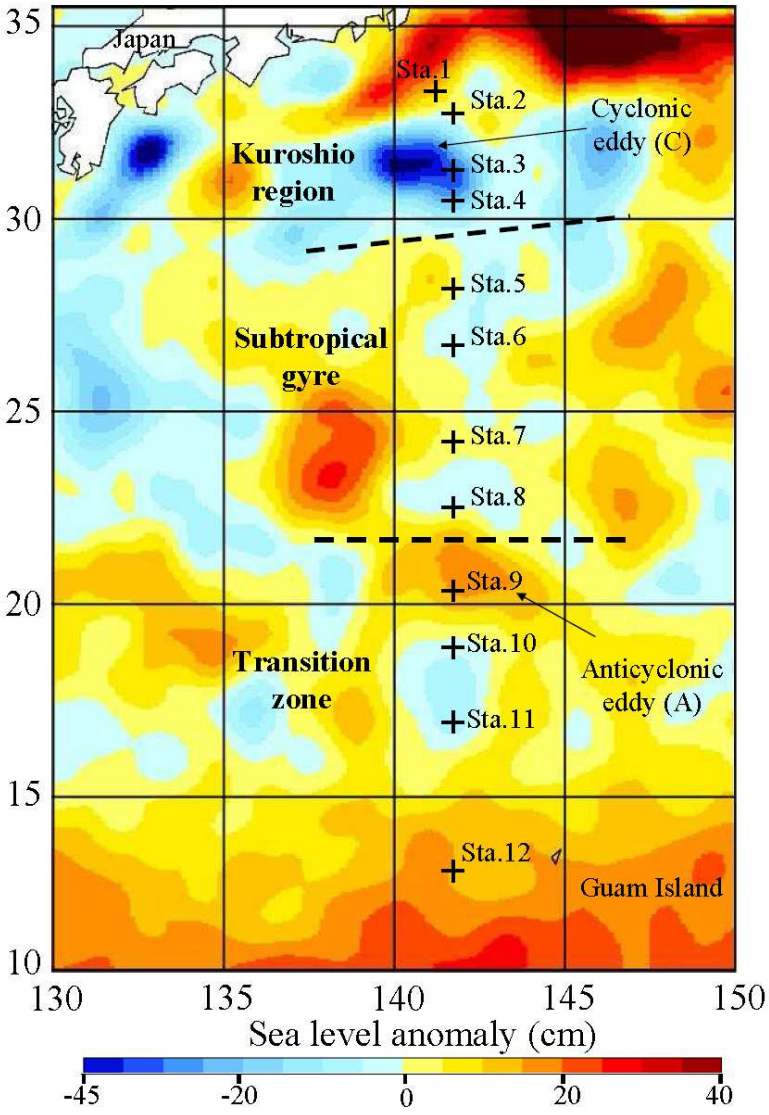

Figure 1: Map of the sea level anomaly (cm) in the west part of the North Pacific subtropical gyre. The sampling stations (black crosses) were separated depending on temperature and salinity into 3 areas: Kuroshio region (stations 1-4), Subtropical gyre (stations 5-8) and the Transition zone (stations 9-12).

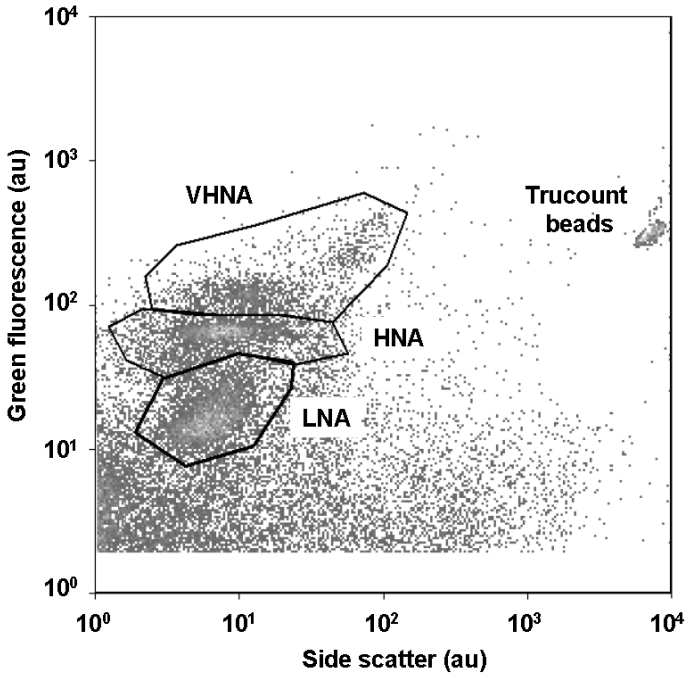

Figure 2: Example of the optical resolution obtained by the analytical flow cytometry of the heterotrophic prokaryote assemblages sampled during the Tokyo-Palau cruise at station 8 (25 m depth). Cytogram of green fluorescence intensity (SYBR Green II ®) versus side scatter intensity showed up three groups of heterotrophic prokaryotes : one defined by prokaryotes with a low nucleic acid content (LNA), one defined by prokaryotes with a high nucleic acid content (HNA) and one defined by those with a very high nucleic acid content (VHNA). Trucount calibration beads (Beckton Dickinson ®) were used both as an internal standard and to determine the volume analysed by the flow cytometer.

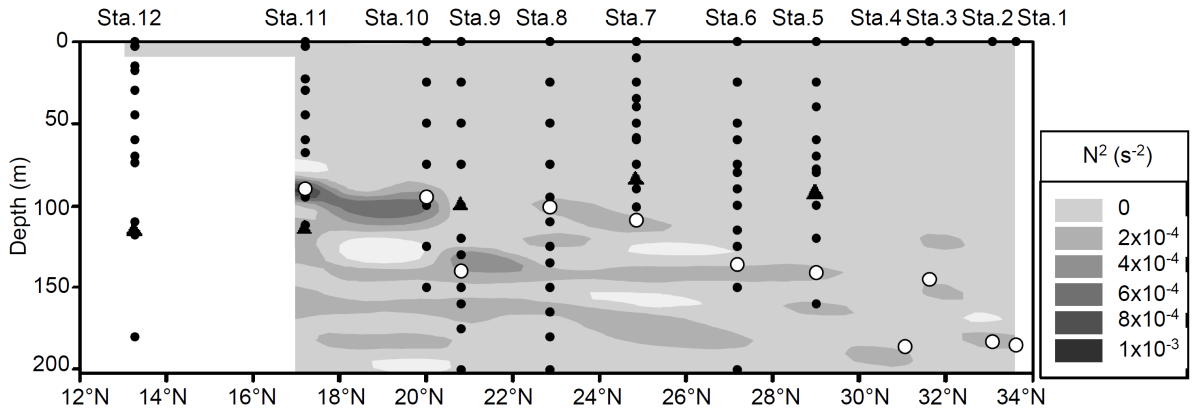

Figure 3: Vertical profiles of the Brunt-Väisäla buoyancy frequency (N^2) calculated from the temperature - salinity measurements. The white circles display the thermocline depth and the black triangles the depths of 1% of photosynthetically active radiation (limit of the euphotic zone).

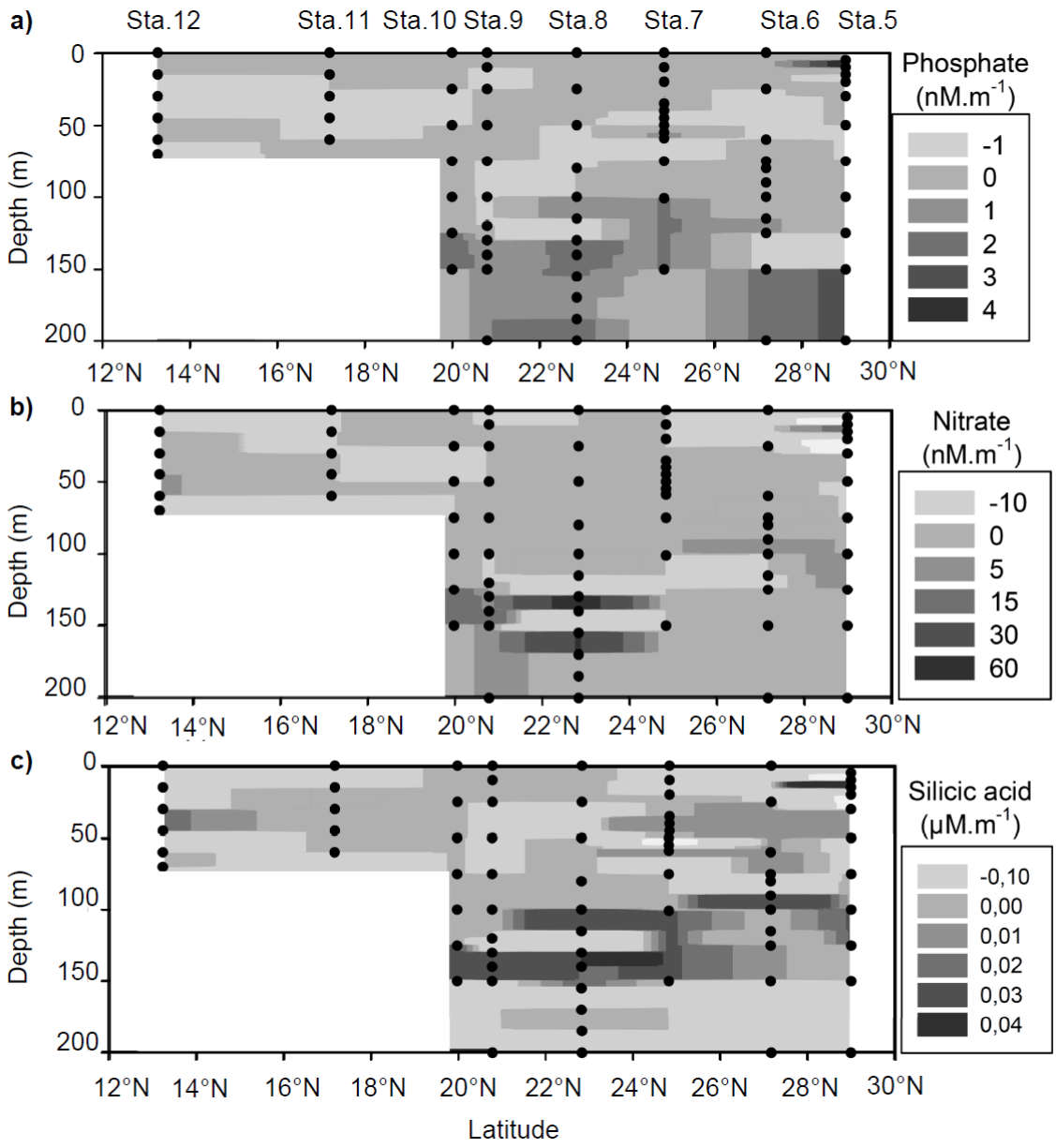

Figure 4: Vertical nutrient gradient (dNutrient/dz) of Phosphate (a), Nitrate (b) and Silicic acid (c), found between station 5 and station 12. The black dots display the sample depths and the names of the stations are indicated in the upper axes.

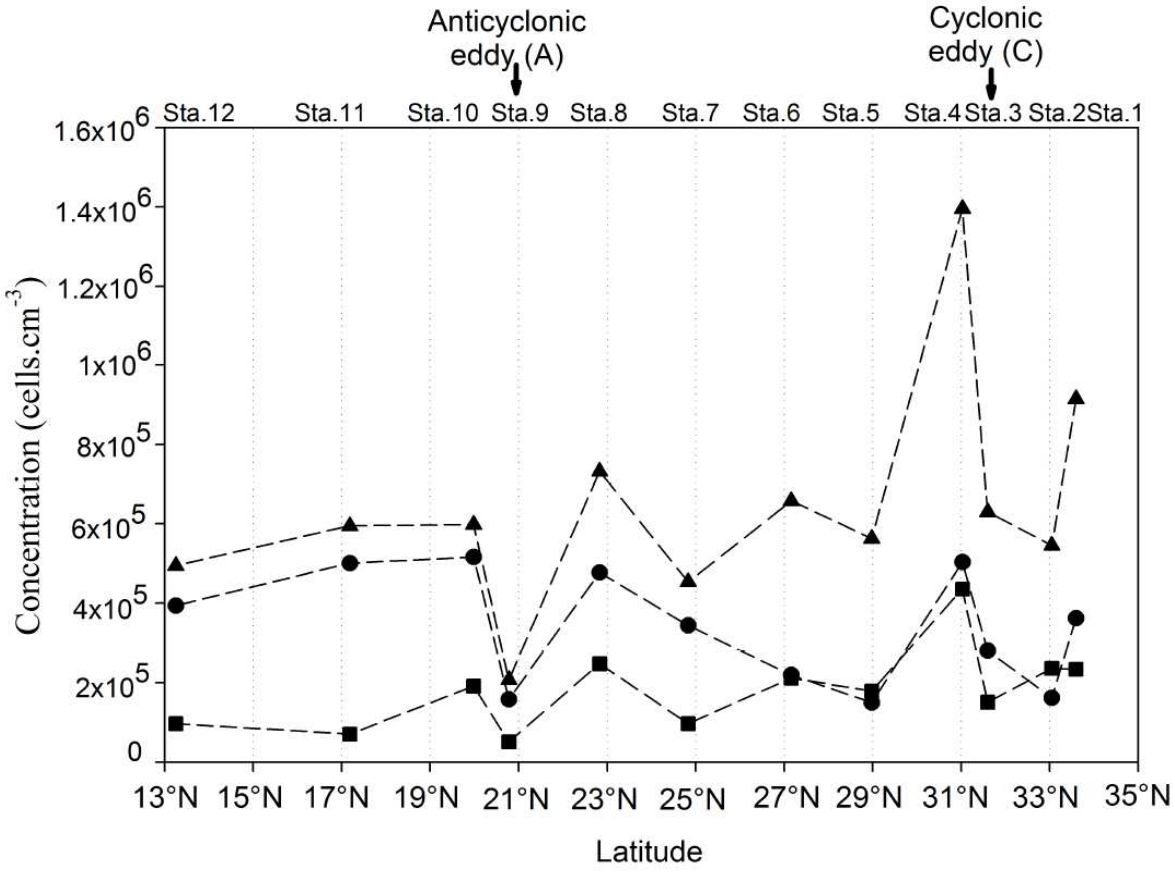

Figure 5: Latitudinal distribution of the heterotrophic prokaryote abundances at the surface along the 141.5°E meridian. (▲) is LNA heterotrophic prokaryotes, (●) the HNA heterotrophic prokaryotes and (■) the VHNA heterotrophic prokaryotes. Sampling stations are indicated on the upper scale axis.

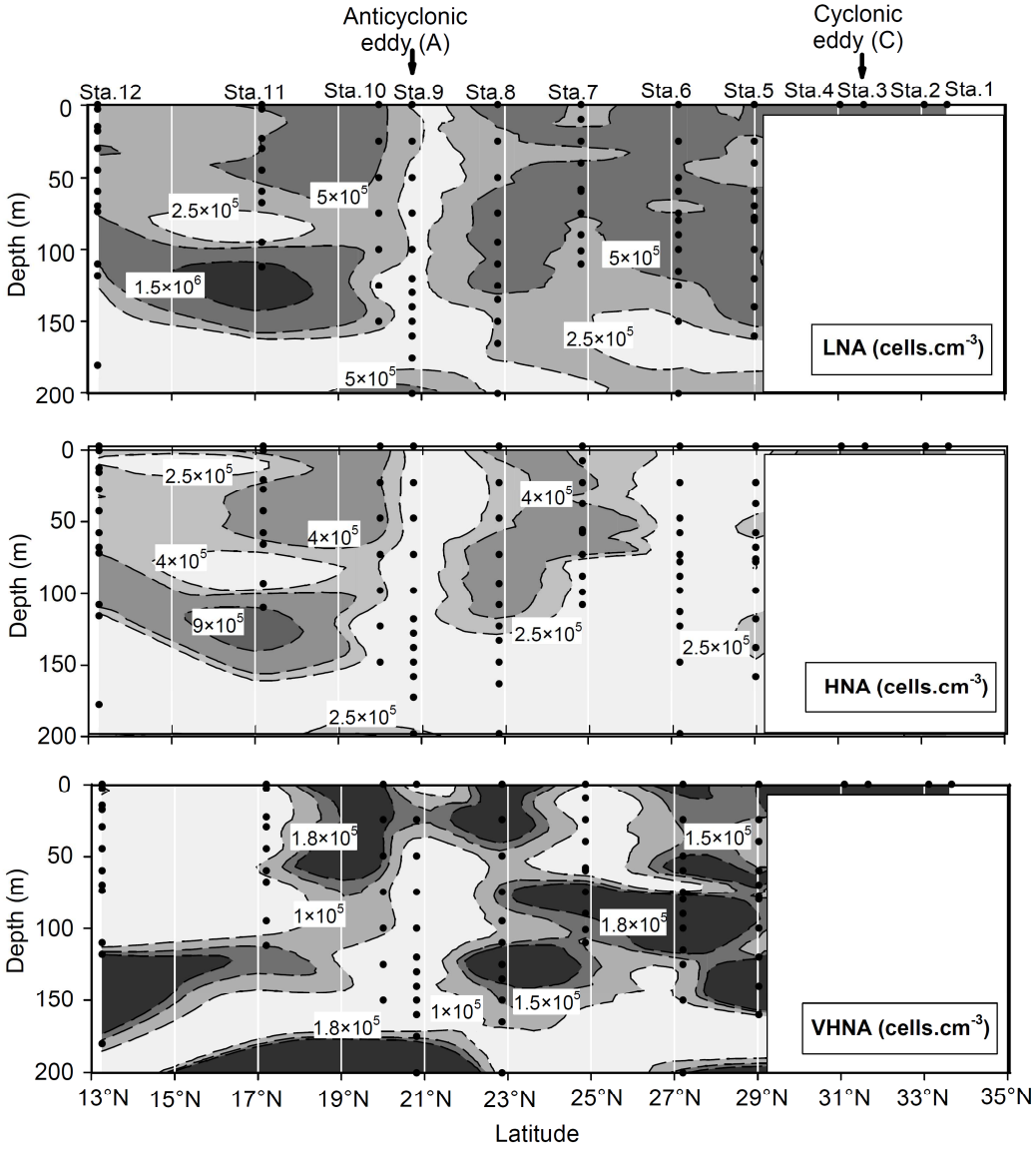

Figure 6: Vertical concentration (cells.cm^{-3}) of LNA, HNA, and VHNA heterotrophic prokaryotes interpolated along the transect during the Tokyo-Palau Cruise. The black dots are the depths sampled.

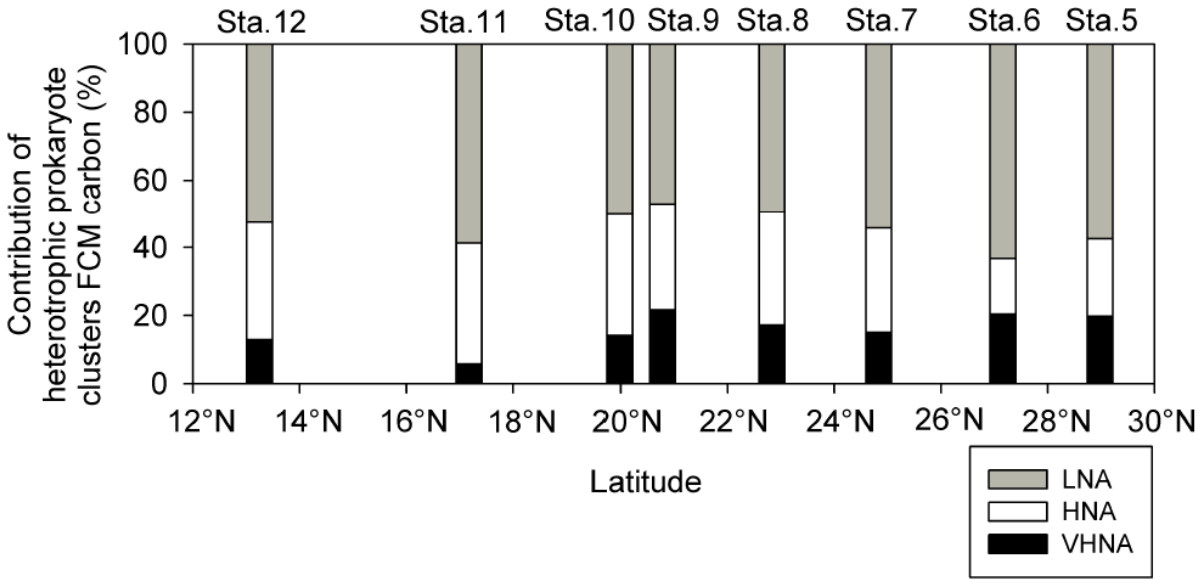

Figure 7: Latitudinal contributions (%) of each heterotrophic prokaryote cluster (LNA, HNA, VHNA) as defined by flow cytometry (FCM) to the whole heterotrophic prokaryote biomass integrated between surface and 200m depth.

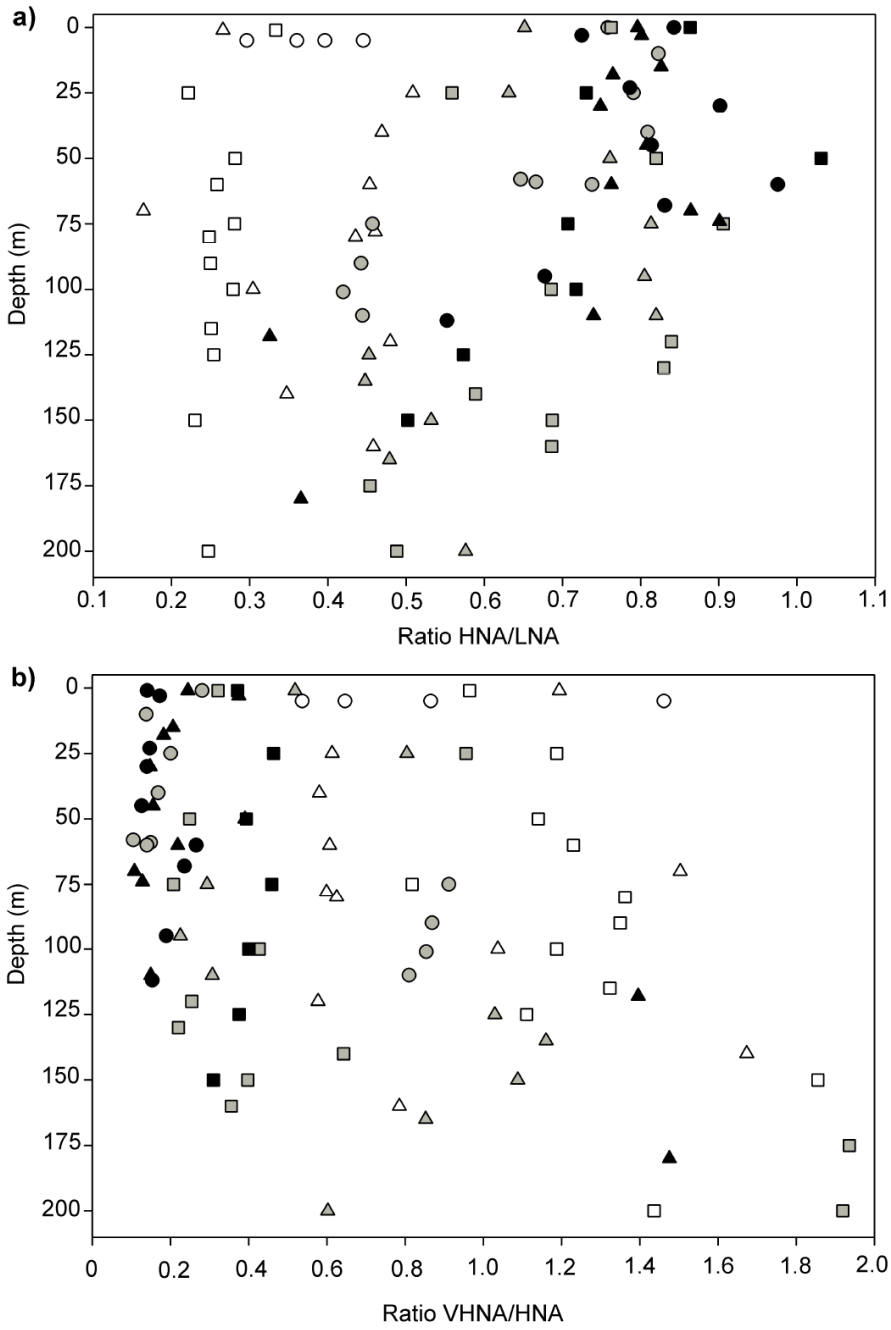

.

Figure 8: Ratios of the abundances between the heterotrophic prokaryote clusters according to depth. a) shows the ratio of the abundances of HNA/LNA clusters while b) shows the ratio of abundances of VHNA/HNA clusters. The white circles are stations 1, 2, 3 and 4. The white triangles and the squares are stations 5 and 6, respectively. The grey circles, triangles, and squares characterize stations 7, 8 and 9, respectively. The black squares, circles and triangles are stations 10, 11 and 12, respectively.

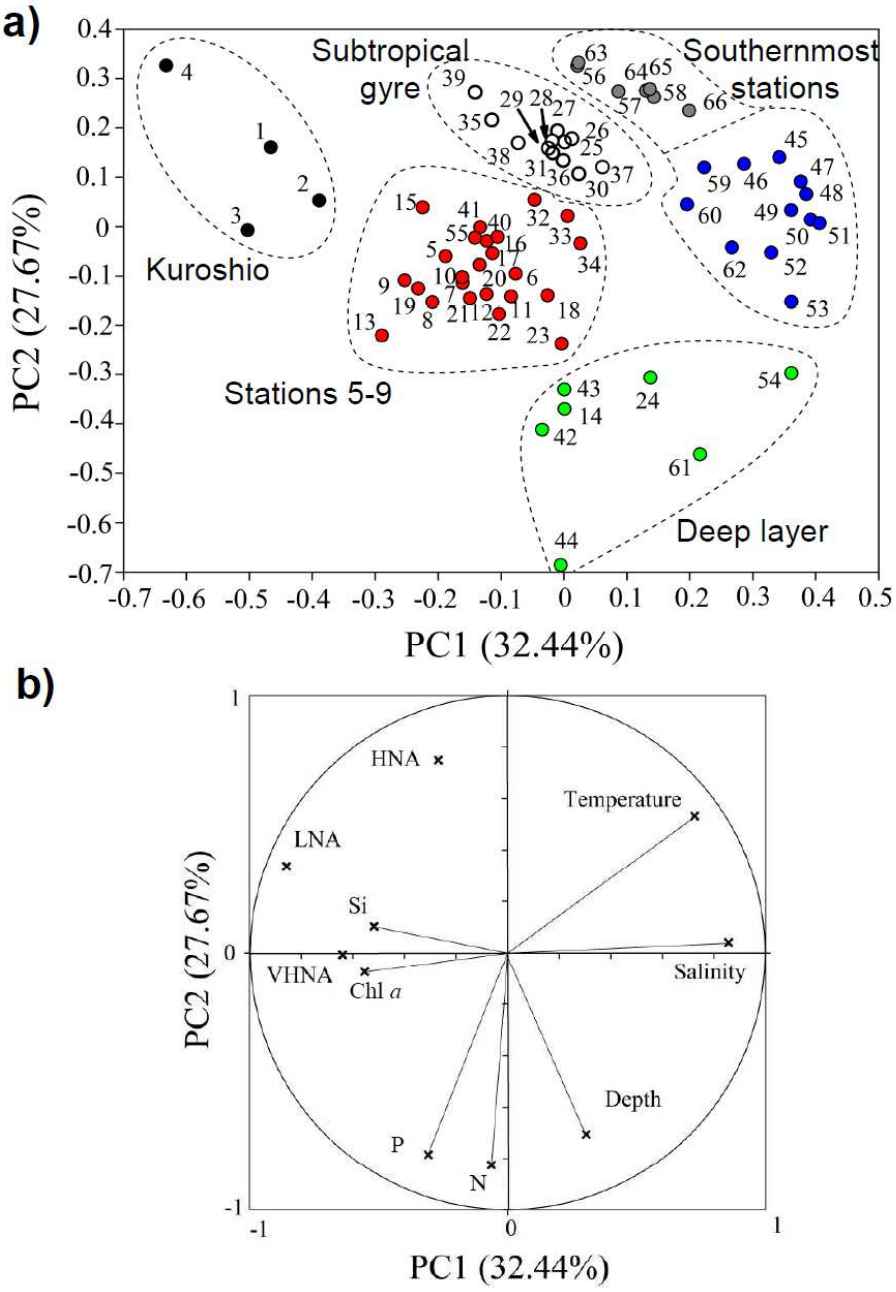

Figure 9: Hierarchical clustering illustrated for the first two principal components of the principal component analysis performed with the data collected from stations 1 to 11 (a). According to the classification (Table 1) the sampling depths (numbers) were discriminated into 6 clusters: one characterizes the Kuroshio region (Cluster 1, black), another incorporates stations 5 to 9 (Cluster 2, red), a third one the deep layer (Cluster 3, green) and the last three clusters characterize the subtropical gyre (Cluster 4, white) and the southernmost stations (5, blue and 6, dark grey). The circle (b) shows the first two dimensions of the principal component analysis. The environmental variables taken into consideration are temperature, salinity, depth, nitrate (N), phosphate (P), silicic acid (Si), and chlorophyll *a* (Chl *a*).

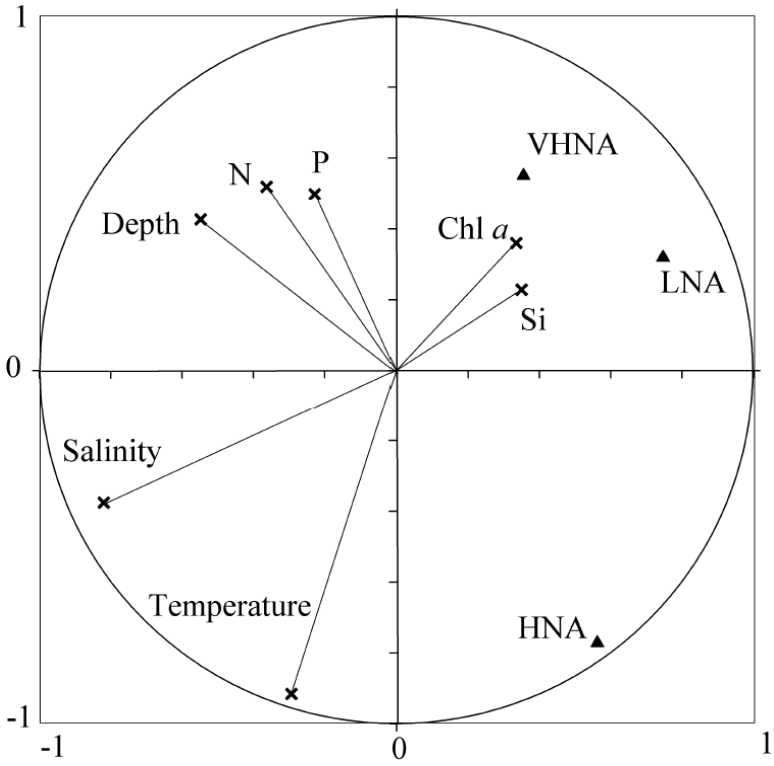

Figure 10: Correlation plot of the redundancy analysis (RDA) on the relationships between the environmental variables and the three subgroups of heterotrophic prokaryotes observed during the cruise (LNA, HNA, VHNA). Chl *a*, N, P, and Si stand for chlorophyll *a*, nitrate, phosphate, and silicic acid, respectively.